MULTIFREQUENCY ABSOLUTE PHASE ESTIMATION VIA GRAPH CUTS

J. Bioucas-Dias and G. Valadão

Instituto de Telecomunicações, Instituto Superior Técnico
Av. Rovisco Pais,1, Torre Norte, 1049-001 Lisboa, Portugal
phone: + (351) 21841846{6,7}, fax: + (351) 218418472, email: {bioucas,gvaladao}@lx.it.pt

ABSTRACT

Many imaging systems, *e.g.*, interferometric synthetic aperture radar (InSAR), yield phase images. These systems retrieve the phase up to a modulo-2π rad ambiguity, *i.e.*, the phase is wrapped into the principal interval $[-\pi\ \pi)$. Phase unwrapping (PU) is, then, a crucial inverse problem to obtain absolute phase, which is what embodies physical information. If the phase difference between neighboring pixels is less than π rad, then, phase unwrapping can be obtained unambiguously. This, however, is not always the case. For example, in InSAR, where absolute phase is proportional to the terrain elevation, we often face neighbor phase differences much larger than π rad. The PU problem is even more challenging for noisy images. This paper proposes a diversity approach, which consists of using two (or more) images of the same scene acquired with different frequencies. Diversity grants an enlargement of the ambiguity interval $[-\pi\ \pi)$, thus, allowing to unwrap images with high phase rates. Furthermore, this paper presents a multi-resolution technique to make denoising. We formulate both tasks as integer optimization problems, which we tackle by using graph cuts techniques. We illustrate the effectiveness of our methodology by showing experimental results, which are, to our knowledge, state-of-the art competitive.

1. INTRODUCTION

There are nowadays many applications based on phase. The generation of digital elevation models, in interferometric synthetic aperture radar (InSAR), and of tissue temperature maps, in magnetic resonance imaging (MRI), are two paradigmatic examples. Imaging systems aimed at phase applications do not have access to the phase itself, but only to its cosine and sine values. These systems can not infer, therefore, the phase, but just its modulo-2π, the so-called interferogram. This sinusoidal nonlinearity, jointly with other degradation mechanisms usually present in phase applications such as noise, high phase rate, and discontinuities, renders absolute phase estimation a hard ill-posed inverse problem.

Diversity is an acquisition strategy where more than one interferogram is acquired, each one corresponding to a different frequency of the sinusoidal nonlinearity. By acquiring more than one interferogram, the number of phase solutions compatible with the observations decreases and, therefore, the hardness of the phase estimation problem is lightened.

Frequency diversity based phase estimation algorithms are scarce. We are aware only of the ones proposed in [1], [2], and [3]. Regarding the first one, it proposes three very simple (and interesting) algorithms that, nonetheless, are error prone. The second one is a multidimensional (accounting for diversity) version of the minimum L^2 norm type of PU algorithm [4], with relaxation to the continuum that is well-known to give rise to solving a Poisson equation [4]. The weaknesses of this approach are long-familiar, in particular the oversmoothing of high phase rate slopes and discontinuities. Concerning the third, it approximates the true surface by means of local planes. The proposed approach requires a simulated annealing computation which is a (nowadays) too much slow optimization technique.

1.1 Contributions

The main contribution of this paper is to present a new algorithm that accomplishes both phase unwrapping and denoising based on diverse observations.

Our approach is Bayesian. The observation model accounts for multiple sinusoidal noisy measurements and the prior is a discontinuity preserving Markov random field (MRF). The absolute phase is inferred by computing the maximum a posteriori (MAP) phase, by exploiting graph-cuts based energy minimization techniques. The algorithm has two main steps:

1. Phase unwrapping: we input two (or more) different frequency interferograms (of the same scene), which provides an extension of the $[-\pi,\pi)$ ambiguity interval and, consequently, an increasing of the phase rates that still allow unwrapping to be a well-posed problem. This frequency *diversity* technique is put forward through a graph-cuts algorithm [6, 5] that minimizes a MRF composed of a sinusoidal data term plus a non-isotropic total variation (TV) prior.
2. Denoising: we achieve denoising by an iterative *multi-precision* MAP-MRF energy minimization graph-cuts algorithm. As in the previous step, (Phase unwrapping), the data term is sinusoidal, while a discontinuity preserving denoising prior is considered [7, 8].

2. PROPOSED FORMULATION

Let $\mathcal{G} = (\mathcal{V},\mathcal{E})$ be an undirected graph associated to a first order Markov random field (MRF), where the set of nodes $\mathcal{V}$ represents image pixels and the set of edges $\mathcal{E}$ represents pairs of neighboring pixels. In this paper the set of edges $\mathcal{E}$ represents horizontal and vertical neighbors.

2.1 Posterior density

We consider, as in, *e.g.*, [9], the observation data model, for each frequency F, to be given by

$$z = e^{jF\phi} + n, \tag{1}$$

where ϕ is the absolute phase[1], n is a complex zero-mean Gaussian circular random variable (*i.e.*, the real and imaginary parts of n are jointly Gaussian, zero-mean, independent and have the same variance). Let us define also the wrapped observed phase, ψ, as

$$\psi = \text{angle}(z). \tag{2}$$

We follow the Bayesian framework. Accordingly, we need to build the posterior density $p(\phi|z)$ of the phase image $\phi \in \mathbb{R}^{|\mathcal{V}|}$ given the observed complex image $z \in \mathbb{C}^{|\mathcal{V}|}$ ($\mathbb{C}$ denotes the complex field). Invoking the Bayes law, we have $p(\phi|z) \propto p(z|\phi)p(\phi)$, where $p(z|\phi)$ is the likelihood function, measuring the data fit and $p(\phi)$ is the prior density encoding *a priori* knowledge about the phase image ϕ.

Let us assume conditional independence in the observation mechanism, *i.e.*, $p(z|\phi) = \prod_{i\in\mathcal{V}} p(z_i|\phi_i)$. Furthermore, let us consider priors such that $\log p(\phi) = -\mu \sum_{(i,j)} V_{ij}(\phi_i - \phi_j)$, where $\mu > 0$ is a scale parameter often termed the regularization parameter, and $V_{ij}(\cdot)$ is the so-called potential associated with edge (ij). In these circumstances, computing the MAP estimate is equivalent to minimize the negative logarithm of the posterior density $E : \mathbb{R}^{|\mathcal{V}|} \rightarrow \mathbb{R} \cup \{+\infty\}$ given by

$$E(\phi) \equiv \underbrace{\sum_{i\in\mathcal{V}} D_i(\phi_i)}_{\text{Data fidelity term}} + \underbrace{\mu \sum_{(i,j)\in\mathcal{E}} V_{ij}(\phi_i - \phi_j)}_{\text{Prior term}}, \tag{3}$$

where $D_i(\phi_i) \equiv -\log p(z_i|\phi_i)$.

Given the observation mechanism, (1) and (2), we have (see e.g. [9])

$$D_i(\phi_i) = -\lambda_i \cos(\phi_i - \psi_i), \quad \text{for } i \in \mathcal{V}, \tag{4}$$

with $\lambda_i \equiv A|z_i|/(2\sigma^2)$ and $\psi_i \equiv \text{angle}(z_i)$, *i.e.*, the loglikelihood function is proportional to a shifted cosine. The MAP absolute phase estimate is then obtained by minimizing the negative of the logposterior function given by

$$E(\phi) \equiv \sum_{i\in\mathcal{V}} -\lambda_i \cos(\phi_i - \psi_i) + \mu \sum_{(i,j)\in\mathcal{E}} V_{ij}(\phi_i - \phi_j). \tag{5}$$

Notice that μ, the regularization parameter, sets the relative weight between the data fidelity and the prior terms.

2.2 Diversity

In this paper we consider frequency diversity. For the sake of simplicity, we take just two frequencies, $F_1 = p/q$ and $F_2 = r/s$, where $\{p,q,r,s\} \in \mathbb{N}$. Assuming that observations (2) are independent for each frequency, the negative loglikelihood is now given by (6)

$$D_i(\phi_i) = -\lambda_{1_i} \cos\left(\psi_{1_i} - F_1\phi_i\right) - \lambda_{2_i} \cos\left(\psi_{2_i} - F_2\phi_i\right), \tag{6}$$

where $\lambda_{1_i}, \lambda_{2_i}$ and ψ_{1_i}, ψ_{2_i} are as in the in the single frequency.

We have already alluded (Section 1.1) to the advantage that frequency diversity gives in extending the $[-\pi\ \pi[$ ambiguity interval. Stating it more clearly, it is easy to show that the sum of two cosine functions, having as in (6) different frequencies $F_1 = p/q$ and $F_2 = r/s$, where $\{p,q\}, \{p,r\}$, $\{q,s\}$, and $\{r,s\}$ are coprime integers[2], results in a third periodic function whose period is $q \times s$; as the initial functions do have periods of respectively q and s, we conclude that the period is, in general, extended and so the ambiguity reduced. This is the "beat production", long known in wave physics. It is a well known behavior, *e.g.*, from wave phenomena, that the greater the beat period extension, the smaller the difference between global and local maxima. Furthermore, it is also well known that beat period extension brings noise amplification. This trade-off should then be taken into account.

2.3 Phase unwrapping with diversity

Introducing the data fidelity term in (6) into (3), we obtain

$$\begin{aligned} E(\phi) \quad &\equiv \quad \sum_{i\in\mathcal{V}} -\lambda_{1_i} \cos\left(\psi_{1_i} - F_1\phi_i\right) - \lambda_{2_i} \cos\left(\psi_{2_i} - F_2\phi_i\right) \\ &+ \quad \mu \sum_{(i,j)\in\mathcal{E}} V_{ij}(\phi_i - \phi_j). \end{aligned} \tag{7}$$

In this section we solve only the phase unwrapping problem. Assuming noiseless environment, there exists a unique couple of integer images, k_1 and k_2, such that the unwrapped (true) phase ϕ is given by

$$F_1\phi = \psi_1 + 2k_1\pi, \tag{8}$$

and

$$F_2\phi = \psi_2 + 2k_2\pi, \tag{9}$$

for two observations with frequencies F_1 and F_2, respectively. By adding (8) and (9) we get

$$\phi = \frac{1}{F_1+F_2}\psi + \frac{2\pi}{F_1+F_2}k, \tag{10}$$

where $\psi \equiv \psi_1 + \psi_2$, and $k \equiv k_1 + k_2$. Then, by introducing (10) into (7) we get

$$\begin{aligned} E(k) \quad &\equiv \quad \sum_{i\in\mathcal{V}} -\lambda_{1_i} \cos\left(\psi_{1_i} - \frac{F_1}{F_1+F_2}(\psi_i + 2k_i\pi)\right) \\ &+ \quad \sum_{i\in\mathcal{V}} -\lambda_{2_i} \cos\left(\psi_{2_i} - \frac{F_2}{F_1+F_2}(\psi_i + 2k_i\pi)\right) \\ &+ \quad \mu \sum_{(i,j)\in\mathcal{E}} V_{ij}\left[(\psi_i - 2k_i) - (\psi_j - 2k_j)\right], \end{aligned} \tag{11}$$

with a correspondingly combinatorial optimization (minimization) to be done on variables k_i $i \in \mathcal{V}$. We take $V\left[(\psi_i - 2k_i) - (\psi_j - 2k_j)\right] = |k_i - k_j|$ the, so-called, non-isotropic total variation (TV). This potential represents the best trade-off between the capability of preserving discontinuities and the computational complexity of minimizing $E(k)$. At this point we make a parenthesis to stress that by adding (8) and (9), we are choosing a symmetrical solution regarding the expression of ϕ in terms of the two frequency diverse observations. Although this choice brings mathematical elegance (because of symmetry), it can be verified that an asymmetrical solution, which can be obtained by formulating (11) as a function of k_1 (or k_2) only, brings shortness of the time of algorithm execution. This is a consequence of allowing a shorter excursion for the k variable. Accordingly, in

[1] We use the term absolute phase to designate the unwrapped phase.

[2] Two integer numbers are said to be coprime if their greatest common divisor is the unity.

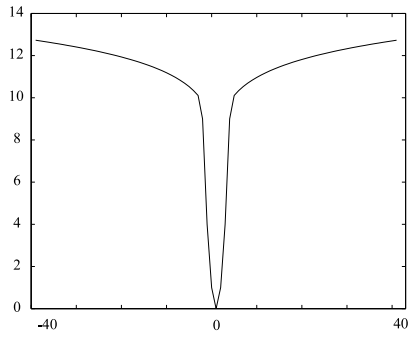

Figure 1: Plot of a half-quadratic potential

the experiments shown in section 4, we have employed such an asymmetrical choice.

We are aware of only two [5], [6] integer optimization algorithms that are able to provide a global minimum for a posterior energy like (11), which is composed by a non-convex data fidelity term and a convex prior potential on the difference of pairs of variables. Herein we refer to [5], as it deals with our non-isotropic TV prior. As long as the energy is a levelable function (see [5]), it is easy to build a source-sink graph such that its min-cut gives the sought global minimizer. For the sake of simplicity we do not describe the graph construction [5]; we just mention that graph min-cuts based algorithms have been proved to be very popular in computer vision, as there are plenty of low-order polynomial complexity algorithms to compute them.

2.4 Denoising with multi-precision

The wrapped phases ψ are noisy. Therefore, even though $\widehat{k}_1$, the estimates of the 2π multiples provided by the PU step, are correct, there is still noise in the absolute phase estimate. For denoising, we take a half quadratic potential type like the one plotted in Fig.1. This potential is quadratic in an origin neighborhood of radius π in order to model Gaussian noise, and with a flat trend elsewhere to preserve discontinuities [10, 11]. We choose the radius of π because we expect to get (most of the) noise wrapped into the interval $[-\pi,\pi($ after the previous phase unwrapping step.

For the sake of clarity, we refer back to the posterior density expression (5), which writes energy as $E \equiv E(\phi)$. Our goal is to compute $\phi^* = \arg\min[E(\phi)]$. We note that the objective function, $E(\phi)$, is non-convex (both in the data fidelity term and in the prior term), which makes this optimization problem very difficult. To circumvent this problem, we discretize the domain of E, using a discretization interval Δ. In doing this, we convert the minimization in $\mathbb{R}^{|\mathcal{V}|}$, where $\mathcal{V}$ denotes the set of pixels, into a combinatorial problem that may be solved efficiently by computing flows on appropriate graphs. We also definitely choose a sub-optimal solution.

We adopt a strategy in which the minimum of E is searched for in a sequence of increasing precisions. This way we both avoid getting stuck in bad local minima (which would be probable, had we started with high precision), and we probably get close to optimization in $\mathbb{R}^{|\mathcal{V}|}$. To this end, let us define $i \in \mathcal{V}$, $\delta_i \in \{0,1\}$, and the sets

$$M^U(\phi',\Delta) \equiv \left\{\phi \in \mathbb{R}^{|\mathcal{V}|} : \phi_i = \phi'_i + \delta_i\Delta\right\}$$
$$M^D(\phi',\Delta) \equiv \left\{\phi \in \mathbb{R}^{|\mathcal{V}|} : \phi_i = \phi'_i - \delta_i\Delta\right\},$$

where $\Delta \in \mathbb{R}$.

Algorithm 1 shows the pseudo-code for our optimization scheme.

Algorithm 1 Multi-precision denoising

Initialization: $\phi = \psi$ {Interferogram}, successup = false, successdown = false
1: **for** $\Delta = 2\pi \times \{2^0, 2^{-1}, \ldots, 2^{-N}\}$ **do**
2: **while** (successup = false OR successdown = false) **do**
3: **if** successup = false **then**
4: $\hat{\phi} = \arg\min_{\hat{\phi} \in M^U(\phi,\Delta)} \tilde{E}(\hat{\phi})$
5: **if** $E(\hat{\phi}) < E(\phi)$ **then**
6: $\phi = \hat{\phi}$
7: **else**
8: successup = true
9: **end if**
10: **end if**
11: **if** successdown = false **then**
12: $\hat{\phi} = \arg\min_{\hat{\phi} \in M^D(\phi,\Delta)} \tilde{E}(\hat{\phi})$
13: **if** $E(\hat{\phi}) < E(\phi)$ **then**
14: $\phi = \hat{\phi}$
15: **else**
16: successdown = true
17: **end if**
18: **end if**
19: **end while**
20: **end for**

Our algorithm engages on a greedy succession of up and down binary optimizations. The precision of the minimization, Δ, starts with the value 2π and ends with the value $2\pi/(2^N)$ where N is a depth of precision. We point out that even if all the computations could have been done with the highest Δ resolution level from the very beginning, choosing this multi-resolution schedule increases dramatically (a logarithmic improvement) the algorithm speed.

To solve the binary optimizations shown in lines 4 and 12 of Algorithm 1, we use the graph-cuts technique presented in [12]. We further add that the $\tilde{E}$ is a majorizer, on the prior terms, of E. So we apply a majorize-minimize (MM) technique such as the one applied in [8]. For details see, *e.g.*, [8, 12]. We stress that we do not have any guarantees of reaching a global minimum with Algorithm 1. This is so because, with generality, we are dealing with both non-convex data fidelity terms and prior terms. However, results in a series of experiments on simulated and real data have been systematically state-of-the art[3].

3. PROPOSED ALGORITHM

The previous sections culminate in our phase imaging algorithm. It consists of a phase unwrapping stage and then denoising. Algorithm 2 shows a simple two lines high level pseudo-code of our phase imaging algorithm.

[3]There are some works, *e.g* [3], that address phase reconstruction and

Algorithm 2 Phase imaging algorithm

1: Do phase unwrapping with diversity
2: Do denoising with multi-resolution

4. EXPERIMENTAL RESULTS

In this section, we briefly illustrate the performance of our algorithm on two representative problems for which phase unwrapping is a hard problem due to high phase rates of the unwrapped images.

Fig. 2 (a) displays an image which is given by a Gaussian having maximum height of 50π rad. Figs. 2 (b) and (c) show the corresponding wrapped images acquired with frequencies $F_1 = 1/2$ and $F_2 = 3/5$, respectively, and having signal-to-noise ratio (SNR $\equiv 1/\sigma_n^2$) of 4 dB. Fig. 2 (d) displays an image of the unwrapped Gaussian, and Fig. 2 (e) a corresponding 3-D rendering. Fig. 2 (f) shows a 3-D rendering after the denoising. It is clear that the algorithm made a perfect phase unwrapping (up to a no-meaning additive constant) for which the diversity information was crucial. The result of the denoising step (ISNR $= 0.0187$ dB) is reflected in Figs. 2 (g) and (h), which show the histograms (the axis are in rad) corresponding to the error of the surfaces rendered in Figs. 2 (e) and (f), respectively. It is noticeable that the denoising erases the secondary modes in the histogram. Fig. 2 (i) is a sheared parabolic ramp having maximum height of 225 rad. Figs. 2 (j) and (k) show the corresponding wrapped images acquired with frequencies $F_1 = 1/4$ and $F_2 = 3/5$ respectively and have SNR $= 7$ dB. Fig. 2 (l) displays an image of the unwrapped sheared parabolic ramp and Fig. 2 (m) a corresponding 3-D rendering. Fig. 2 (n) shows a 3-D rendering after the denoising. Figs. 2 (o) and (p) show the histograms (the axis are in rad) corresponding to the error of the surfaces rendered in Figs. 2 (m) and (n), respectively. Again the algorithm made a perfect phase unwrapping for which the diversity information was crucial. We emphasize that the unwrapping preserves the discontinuity between the horizontal and the parabolic ramps. Concerning the denoising step (ISNR $= 5.4792$ dB), it is noticeable that the denoising erases the secondary modes in the first histogram.

Still referring to the histograms, the ones corresponding to the noisy images show, in general, a multi modal shape. Besides the central mode, there are some secondary modes departed around multiples of -2π and 2π from the center. Those correspond to "spikes" as a result of the data observation model. After denoising they do disappear. We further note that each final result was obtained in a few dozens of seconds in a 3.0 GHz Intel PC. Furthermore all the free parameters were hand tuned in order to get the best results.

5. CONCLUDING REMARKS

We have proposed a (discontinuity preserving) denoising Bayesian algorithm to phase unwrapping; to achieve phase unwrapping we propose a diversity technique, while denoising is to be dealt with by employing multi-precision. Among the scientific community there is still an alive debate of whether denoising should be done after phase unwrapping, before phase unwrapping, or any other solution in-between. In this paper, we have chosen the first option in order to avoid the denoising step to corrupt the phase unwrapping process. Our approach is a MAP-MRF one. We have chosen both non-convex data fidelity and prior potential terms, in the MRF, so there is no hope to find the global minimum efficiently. Thus, we propose a sub-optimal minimization algorithm.

The experimental results are encouraging; to our knowledge they are state-of-the-art.

In the future we intend to develop learning schemes for the selection of the best prior parameter μ, given some absolute phase estimation problem, and get a deeper understanding of noise in the multi-frequency scenario.

deal with high phase rates; however they do employ simulated annealing.

REFERENCES

[1] W. Xu, E. Chang, L. Kwoh, H. Lim, and W. Heng. Phase-unwrapping of sar interferogram with multi-frequency or multi-baseline. In *Proceedings of the 1994 International Geoscience and Remote Sensing Symposium-IGARSS'94*, vol. 2, pp 730–732, 1994.

[2] M. Vinogradov and I. Elizavetin. Phase unwrapping method for the multifrequency and multibaseline interferometry. In *Proceedings of the 1998 International Geoscience and Remote Sensing Symposium-IGARSS'98*, vol. 2, pp. 1103–1105, 1998.

[3] V. Pascazio and G. Schirinzi. Multifrequency insar height reconstruction through maximum likelihood estimation of local planes parameters. *IEEE Transactions on Image Processing*, vol. 11, pp. 1478–1489, 2002.

[4] D. Ghiglia and M. Pritt. *Two-Dimensional Phase Unwrapping. Theory, Algorithms, and Software*. John Wiley & Sons, New York, 1998.

[5] J. Darbon and M. Sigelle. Image restoration with discrete constrained total variation part ii: Levelable functions, convex priors and non-convex cases fast and exact optimization. *Journal of Mathematical Imaging and Vision*, pp. 277–291, 2006.

[6] H. Ishikawa. Exact Optimization for Markov Random Fields with Convex Priors. *IEEE Transactions on Pattern Analysis and Machine Intelligence*, vol. 25, no. 10, pp. 333–1336, 2003.

[7] C. Bouman and K. Sauer. A generalized Gaussian image model for edge-preserving MAP estimation. *IEEE Transactions on Image Processing*, vol. 2, no. 3, pp 296–310, 1993.

[8] J. Bioucas-Dias and G. Valadão. Phase unwrapping via graph cuts. *IEEE Transactions on Image Processing*, vol. 16, no. 3, pp 698–709, 2007.

[9] J. Dias and J. Leitão. The $\mathbb{Z}\pi$M algorithm for interferometric image reconstruction in SAR/SAS. *IEEE Transactions on Image Processing*, vol 11, pp. 408–422, 2002.

[10] S. Z. Li. *Markov Random Field Modeling in Computer Vision*, volume 9 of *Computer Science Workbench*. Springer-Verlag, New York, 1995.

[11] M. Rivera and J. Marroquin. Half-Quadratic Cost Functions for Phase Unwrapping. *Optics Letters*, vol. 29, no. 5, pp 504–506, 2004.

[12] V. Kolmogorov and R. Zabih. What energy functions can be minimized via graph cuts? *IEEE Transactions on Pattern Analysis and Machine Intelligence*, vol. 26, no. 2, pp. 147–159, 2004.

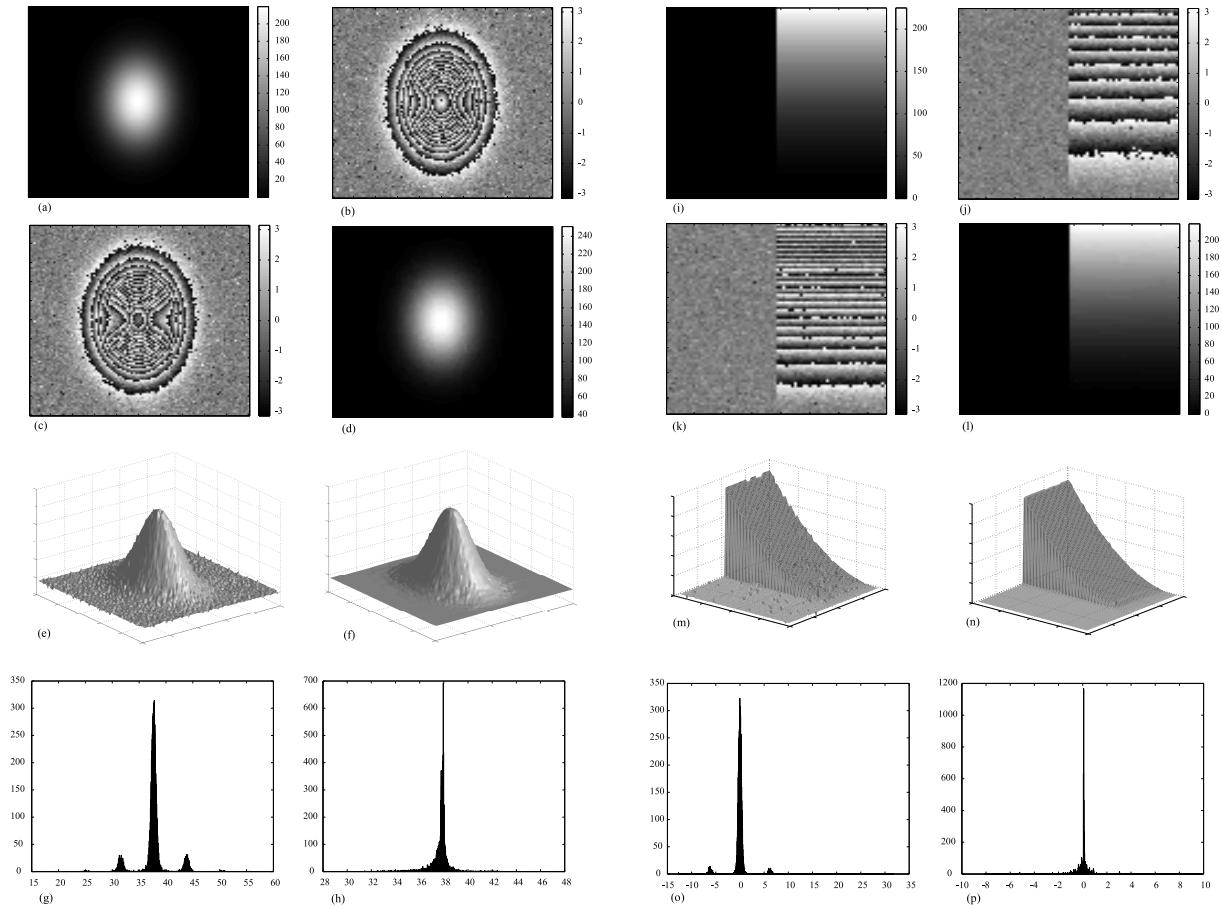

Figure 2: (a) Original Gaussian phase image. (b) Image in (a) wrapped with a relative frequency of $1/2$. (c) Image in (a) wrapped with a relative frequency of $3/5$. (d) Unwrapped image from the previous wrapped images shown in (b) and (c). (e) 3-D rendering of the image in (d). (f) 3-D rendering of the image in (d) after the denoising step. (g) Histogram corresponding to the error of the surface rendered in (e). (h) Histogram corresponding to the error of the surface rendered in (f). (i) Original sheared quadratic ramp phase image. (j) Image in (i) wrapped with a relative frequency of $1/4$. (k) Image in (i) wrapped with a relative frequency of $3/5$. (l) Unwrapped image from the previous wrapped images shown in (j) and (k). (m) 3-D rendering of the image in (l). (n) 3-D rendering of the image in (l) after the denoising step. (o) Histogram corresponding to the error of the surface rendered in (m). (p) Histogram corresponding to the error of the surface rendered in (n).